I R A M P
3(1), June 2012, pp. 61-73

ISSN: 2229-3159

Broadening of Resonance Induced by High-order Spatial Harmonics

O. V. BELAI[1] AND D. A. SHAPIRO[1,2]

[1]Institute of Automation and Electrometry, Siberian Branch, Russian Academy of Sciences
1 Koptjug Avenue, Novosibirsk, 630090 Russia
[2]Novosibirsk State University, 2 Pirogov Street, Novosibirsk 630090, Russia

ABSTRACT: Coherent preparation of quantum states of atoms and ions by laser light can lead to electromagnetically induced transparency and related effects. In particular, the standing wave at the adjacent transition induces a new type of nonlinear resonance in the probe-field spectrum of a three-level system. The resonance is due to the effect of high-order harmonics of atomic coherence. However, the resonance is broadened in experiment and the reason of the broadening was unclear. The paper describes how the velocity changing collisions broaden the resonance. The analytic theory taking into account up to 4-th order of the perturbation theory is presented. The numerical solution of density matrix equations is discussed. The analytical formulas are shown to describe the experiment qualitatively while the numerical computation demonstrates quantitative agreement. The Coulomb dephasing is shown to be the physical mechanism of the broadening.

PACS numbers: 32.70.Jz,42.50.Gy,42.50.Hz,52.20.Hv

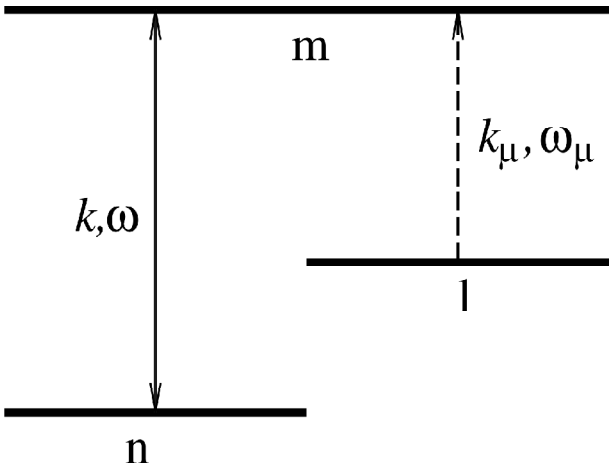

Figure 1: Level diagram: strong standing wave (solid line with two arrows) with frequency and wavevector ω, k and probe wave ω_μ, k_μ (dashed with one arrow)

I. INTRODUCTION

It is well-known that the light absorption in the atomic medium near a resonant frequency can be reduced substantially or even canceled with the help of strong driving field at the adjacent transition due to the splitting of levels. This effect, so-called electromagnetically induced transparency (EIT) [1, 2], is a base of quite a number of atomic coherence effects, in particular, the resonant enhancement of electro-optical processes [3–5], the lasing without inversion [6], suppression of two-photon absorption [7]. Under conditions of EIT the super-narrow resonances arise leading to the giant dispersion within the transparency window. This property is helpful for light deceleration [8–10] and makes the effect promising for application in the frequency standards [11], the precision magnetometery [12], and as a storage of quantum information [13–15].

As a rule, in EIT experiments three-level Λ-systems interact with the probe and driving fields presented by running waves [16, 17]. A finite analytical expression for the probe field absorption at high intensity of the driving field cannot be derived even for rare collisionless gas. Higher spatial harmonics are taken into account by the Feldman — Feld continuous fractions [21]. This expression was obtained from the known continuous fraction for populations in two-level system in bichromatic field [27, 28]. In the case of equal relaxation constants and exact resonance the populations can be expressed in terms of the rapidly oscillating Bessel function [29] (see also the survey by Stenholm [30]).

In experiment the higher spatial harmonics were studied in cadmium spectrum. Atoms interacted with two counterpropagating waves of different frequency and amplitude [31, 32] (see also [33]). Under the frequency scanning the subradiative structure was observed in the absorption spectrum that included up to 5 peaks that became more frequent in the line center (so called "1/*n*-resonances"). Herewith the spectrum appeared to be very sensitive to the ratio of amplitudes of the waves, especially in the case of close amplitudes.

Theoretical and experimental study of the standing wave as the driving field was carried out [18, 19] in Λ-configuration, Fig. 1. Strong field was generated on laser transition **ArII** $mn = 4p^2S_{1/2} - 4s^2P_{1/2}$ at wavelength $\lambda = 458$nm. Probe field was a running wave at $ml = 4p^2S_{1/2} - 3d^2P_{3/2}$, $\lambda_\mu = 648$nm. The absorption of probe field was measured as a function of detuning $\Delta = \omega - \omega_{mn}$. At the specific probe field detuning $\Delta_\mu = k_\mu\Delta / k$ the well known EIT resonance was observed. Along with it a new structure at $\Delta_\mu = 0$ was discovered and its position in the spectrum was independent of the strong field detuning Δ, as shown in Fig. 2.

At $\Delta = 0$ the positions of both resonances coincide but their widths and signs differ. The new structure looks like peak of the electromagnetically induced transparency split by narrow dip. At higher strong field detuning Δ the dip is transformed into a peak at the center $\Delta_\mu = 0$. The new structure was observed for non-typical situation with a wide lower level *n*, where the forbidden transition was wider than the allowed one $\Gamma_{nl} >> \Gamma_{ml}$. Previously the opposite limiting case $\Gamma_{nl} << \Gamma_{\mathrm{ml}}$ was studied in details. For this reason the motionless structure was overseen both in the perturbation theory [20] and in numerical calculations [21]. This structure is originated by the higher harmonics at transitions *ml* and *nl* induced by the standing wave.

Since the spatial modulation of coherence arises at simultaneous action of two counterpropagating running waves the effect is maximal for particles with zero projection of the velocity vector onto the wavevector. Atoms or ions near the nodes of the standing wave do not feel the strong field. Thereafter, the EIT (or absorption) induced by the strong field considerably decreases near zero probe field detuning $\Delta_\mu = 0$. For the same reason the resonance of slow atoms is not sensitive to the Doppler broadening and appears to be sufficiently narrow. The small width of the resonance leads to sharp slope of the dispersion curve then the resonance is suitable for experiments on slow light or other EIT applications.

The theory for collisionless case is based on the continuous fraction averaging over the velocity distribution. Fig. 3 shows the collisionless theory of resonances. Comparison with Fig. 2 demonstrates a good agreement in positions of both resonances. At the same time the width of observed slow-atom resonance appears to be several times wider than the prediction of collisionless theory. It is naturally to assume that the broadening is a result of the Coulomb scattering of excited ions by the ground state ions in plasma. In general theory of Coulomb scattering [22] the higher harmonics of spatial coherence are neglected. The neglecting is valid for the Lamb dip in two-level system where the oscillation of populations is smoothed out at the averaging over velocities. The theory is also valid for running wave in three-level system. Calculation of the shape of known EIT resonance at $\Delta_\mu = k_\mu\Delta / k$ in the three-level system under the field of running wave demonstrates a good agreement with experiment. It was shown that the resonance is caused by the Bennet dip in the population distribution over velocity. Its width becomes nearly 3 times greater than in collisionless case [23]. For the new resonance $\Delta_\mu = 0$ the theory taking the scattering into account was absent. Only a rough estimation of the Coulomb dephasing effect had been presented in paper [24] under the approximation of empty intermediate level *m*.

The aim of the present paper is to explain how the collision broadening occurs. The key equations of the broadening theory of the resonance of higher spatial harmonics are presented below, while the specific details of

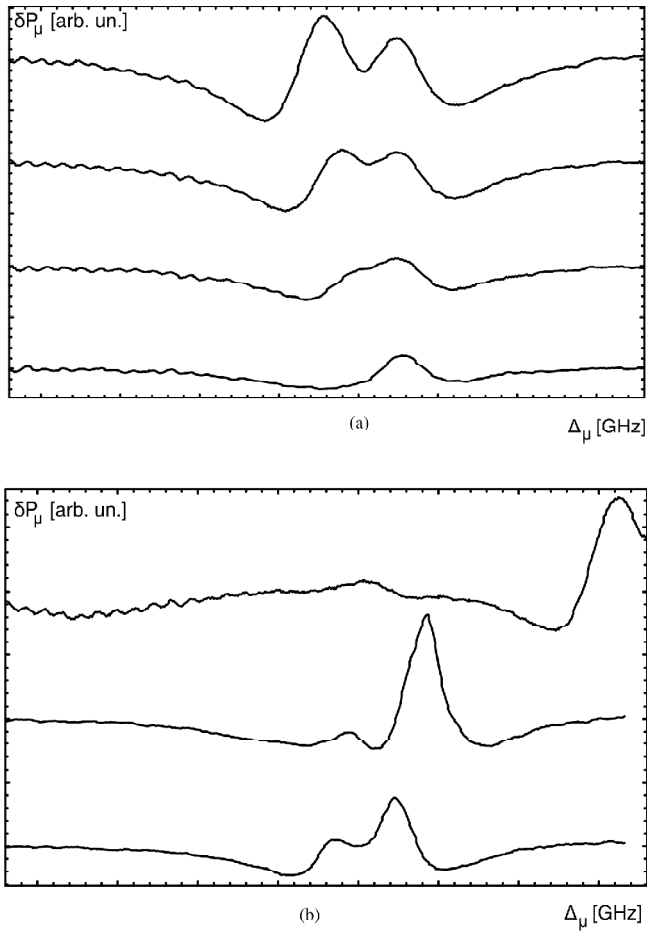

Figure 2: Measured spectra. (a) At Δ = 0 and different Rabi frequencies: from bottom up Ω = 0, 50, 75, and 100 MHz. (b) At Ω = 100 MHz and different detuning: from bottom Δ = 0.2, 0.7, and 2 GHz. The amplitude of the last curve is doubled

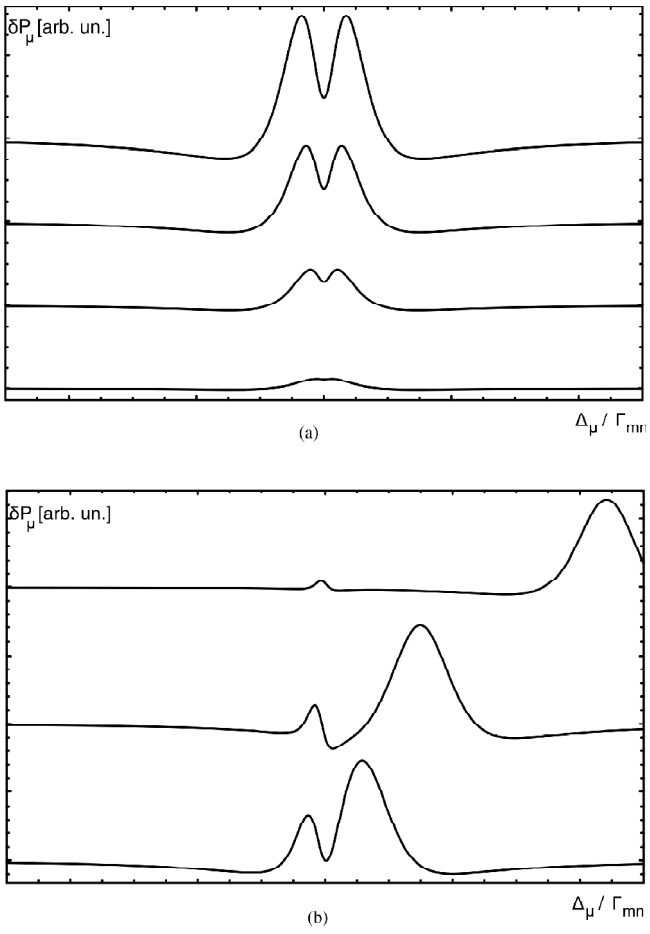

Figure 3: Calculated spectra. (a) At Δ = 0, kv_T = 20 Γ_{mn}, Γ_{ml} / Γ_{nl} =1/6, $\Gamma_{mn} \approx \Gamma_{nl}$ and different Rabi frequencies: from bottom up Ω / Γ_{mn} = 0.1, 0.2, 0.3, and 0.4. (b) At Ω / Γ_{mn} = 0.4 0 and different detuning: from bottom up Δ / Γ_{mn} = 0.7, 2.2, and 6.6

numerical and analytical calculation can be found in papers [25, 26]. The account of collisions is important not only for the quantitative interpretation of experiments in argon discharge plasma. The velocity changing collisions could broaden the resonances and decrease the slope of dispersion curve in other experiments on EIT with other gas media where the field of standing wave is exploited.

II. PERTURBATION THEORY

Let us consider the gas of three-level systems under the driving field of standing wave, Fig. 1 including the collisions. At weak saturation the solution can be obtained as a perturbation series. The second order of the perturbation series does not include the effects of higher spatial harmonics. The second harmonics manifests itself only in the fourth order, then we restrict ourselves by the fourth order of the perturbation expansion following [25].

(A) Equation for Density Matrix

The density matrix ρ_{ij} equation describes the interaction of three-level system with parallel driving and probe waves

$$i\,(\Gamma_{ij} + \partial_t + v\partial_x)\,\rho_{ij} = [V, \rho]_{ij}. \tag{1}$$

Here Γ_{ij} are the relaxation constants, t is time, x is the coordinate along the direction of the wavevectors $k \| k_\mu$ of the driving and probe waves, v is the projection of the velocity vector to this common direction, $\hat{V} = -\mathbf{E}\cdot\hat{\mathbf{d}}/2\hbar$ is the

operator of dipole interaction, $\hat{\mathbf{d}}$ is the dipole moment operator, $\hbar$ is the Plank constant, $\mathbf{E}$ is the electric field of the light wave, indices i, j posses the values l, m, n, square brackets denote the commutator. Coupled equations for polarizations ρ_{ml} and ρ_{nl} of the allowed and forbidden transitions follow from (1):

$$i(\Gamma_{ml} + \partial t + v\partial_x)\,\rho_{ml} = V_{ml}\rho_{ll} + V_{mn}\rho_{nl} - \rho_{mm}V_{ml},$$
$$i(\Gamma_{nl} + \partial_t + v\partial_x)\,\rho_{nl} = V_{nm}\rho_{ml} - \rho_{nm}V_{ml}. \tag{2}$$

We neglect the population ρ_{mm} of level m and polarization ρ_{nm} being small under experimental conditions. The equilibrium distribution at level l is Maxwellian

$$\rho_{ll} = N_l(v) = N_l v_T^{-1}\pi^{-1/2}e^{-v^2/v_T^2},$$

where $v_T = \sqrt{2T/M}$ is the thermal velocity, T is the temperature in energetic units, M is the mass of the radiating particle. Let us specify the fields of running and standing waves in the form:

$$\mathbf{E}_\mu(x,t) = \frac{1}{2}\mathbf{E}_\mu^0 e^{ik_\mu x - i\omega_\mu t} + c.c.,\ \mathbf{E}(x,t) = \mathbf{E}^0\cos kx\, e^{-i\omega t} + c.c., \tag{3}$$

where $\mathbf{E}^0$ and $\mathbf{E}_\mu^0$ are the amplitudes, c.c. denotes the complex conjugated terms. Let Rabi frequencies of the driving and probe field be $\Omega_\mu = \mathbf{E}_\mu^0 \cdot \mathbf{d}_{ml}/2\hbar$, $\Omega = \mathbf{E}^0 \cdot \mathbf{d}_{mn}/2\hbar$ where $\mathbf{d}_{ij}$ are matrix elements of the dipole moment.

Changing the variables in equation (2):

$$\rho_{ml} = \rho_\mu(x, v)\exp(ik_\mu x - i\Delta_\mu t),\ \rho_{nl} = \rho_v(x, v)\exp(ik_\mu x + i\Delta t - i\Delta_\mu t),$$

we get a closed steady state equation set for amplitudes ρ_μ and ρ_v of polarizations at allowed and forbidden transitions:

$$(\Gamma_\mu - i\Delta_\mu + ik_\mu v + v\partial_x)\,\rho_\mu = -2i\Omega\cos(kx)\rho_v + i\Omega_\mu N_l(v),$$
$$(\Gamma_v + i\Delta - i\Delta_\mu + ik_\mu v + v\partial_x)\rho_v = 2i\Omega^*\cos(kx)\rho_\mu, \tag{4}$$

where $\Gamma_\mu = \Gamma_{ml}$, $\Gamma_v = \Gamma_{nl}$.

These equations take into account only interaction of ions with light, however the Coulomb ion-ion scattering strongly affects the probe-field spectrum. The Coulomb scattering is small-angle then it can be described as a diffusion process in the velocity space. The scattering is independent of the ionic internal quantum state, then it can be described by operator $\hat{S} = D\partial_{vv}$ in the right sides of Eqs. (1), (2), (4), where

$$D = \frac{\nu v_T^2}{2},\ \nu = \frac{16\sqrt{\pi}NZ^2e^4\Lambda}{3M^2v_T^3}. \tag{5}$$

Here D is the diffusion coefficient, ν is the effective transport frequency of ionic collisions, Ze is the ion charge, Λ is the Coulomb logarithm, N is the ionic density [22]. The full ionic density enters into expression (5), since the concentration of excited ions is small, and then the excited ions are scattered mainly by the ions in the ground state.

(B) Nonlinear Absorption Spectrum

Since the solutions to (1) are periodic functions of coordinate, the density matrix elements $\rho(x)$ are Fourier series over the spatial harmonics

$$\hat{\rho}(x,v) = \sum_{p=-\infty}^{\infty}\hat{r}_p(v)e^{ipkx}. \tag{6}$$

Nonlinear absorption spectrum is defined as the difference between probe-field absorption spectra when the driving field is turned off and turned on

$$\delta\mathcal{P}_\mu = \mathcal{P}_\mu(0) - \mathcal{P}_\mu(\Omega), \quad \mathcal{P}_\mu \propto \mathrm{Im} \int_{-\infty}^{\infty} r_{ml,0}(v)\, dv. \tag{7}$$

Its advantage is absence of the broad Doppler contour being subtracted, as shown in Fig. 4. Scales of axis y for linear and nonlinear absorption differs by an order of magnitude, then the nonlinear spectrum is better to study small nonlinear contributions of the strong driving field. Expression for $\delta\mathcal{P}_\mu$ includes only zeroth Fourier component of the polarization $r_{ml,0}(v)$, since one must average the absorption over coordinate x and other terms in series (6) give no contribution.

Fig. 5 shows $\delta\mathcal{P}_\mu$ as a function of the detuning Δ_μ at different strong-field amplitude Ω and detuning Δ. The absorption is plotted using cumbersome formulas for the 4th order perturbation theory [25], then they take into account only the second spatial harmonics. The parameters of discharge plasma and laser radiation were chosen close to experimental. The left column shows the resonance case $\Delta = 0$. The amplitude of standing wave increases top-down. The peak is sharp in the upper plot, then its top becomes fiat, and split at last. The dip appears corresponding to the studied effect of the second spatial harmonics. In the right-hand column the amplitude is constant whereas the strong-field detuning increases top-down. The top plot in the second column coincides with the bottom plot in the first column. Then the resonance moves to the right with increase in detuning Δ while the second less pronounced peak stays at the line center $\Delta_\mu = 0$. Plots demonstrate how the dip turns into the peak with increasing in the detuning.

The dip or peak is broaden compared to the collisionless case. The broadening due to velocity changing collisions could depend only on the diffusion coefficient and the wavenumber $k_\mu \sim k$. There is only one combination with the dimension of frequency $\delta\Delta_\mu \sim D^{1/3} k^{2/3} \sim \nu^{1/3}(kv_T)^{2/3}$. To test the hypothesis we plotted the series of curves $\delta\mathcal{P}_\mu(\Delta_\mu)$,

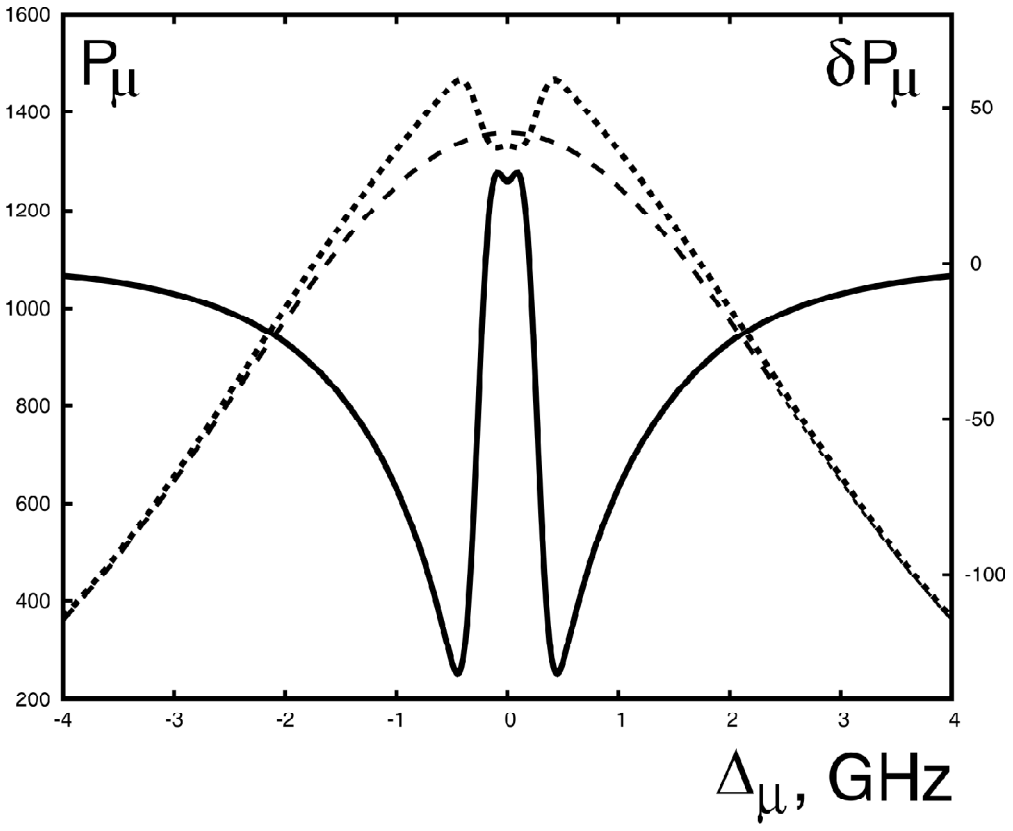

Figure 4: Absorption $\mathcal{P}_\mu(\Omega)$ (arb. units) as a function of the probe-field frequency detuning Δ_μ (dots), the same without the strong field $\mathcal{P}_\mu(0)$ (dashes); the ordinate axis is at the left. Their difference $\delta\mathcal{P}_\mu$, the spectrum of nonlinear absorption (solid curve); the ordinate axis is at the right

Fig. 6, at different diffusion coefficients. The full width at half maximum (FWHM) as a function of D is shown in the inset. The slope 0.31 is obtained by the least square fitting in agreement with estimated exponent 1/3. This dependence has a simple physical explanation.

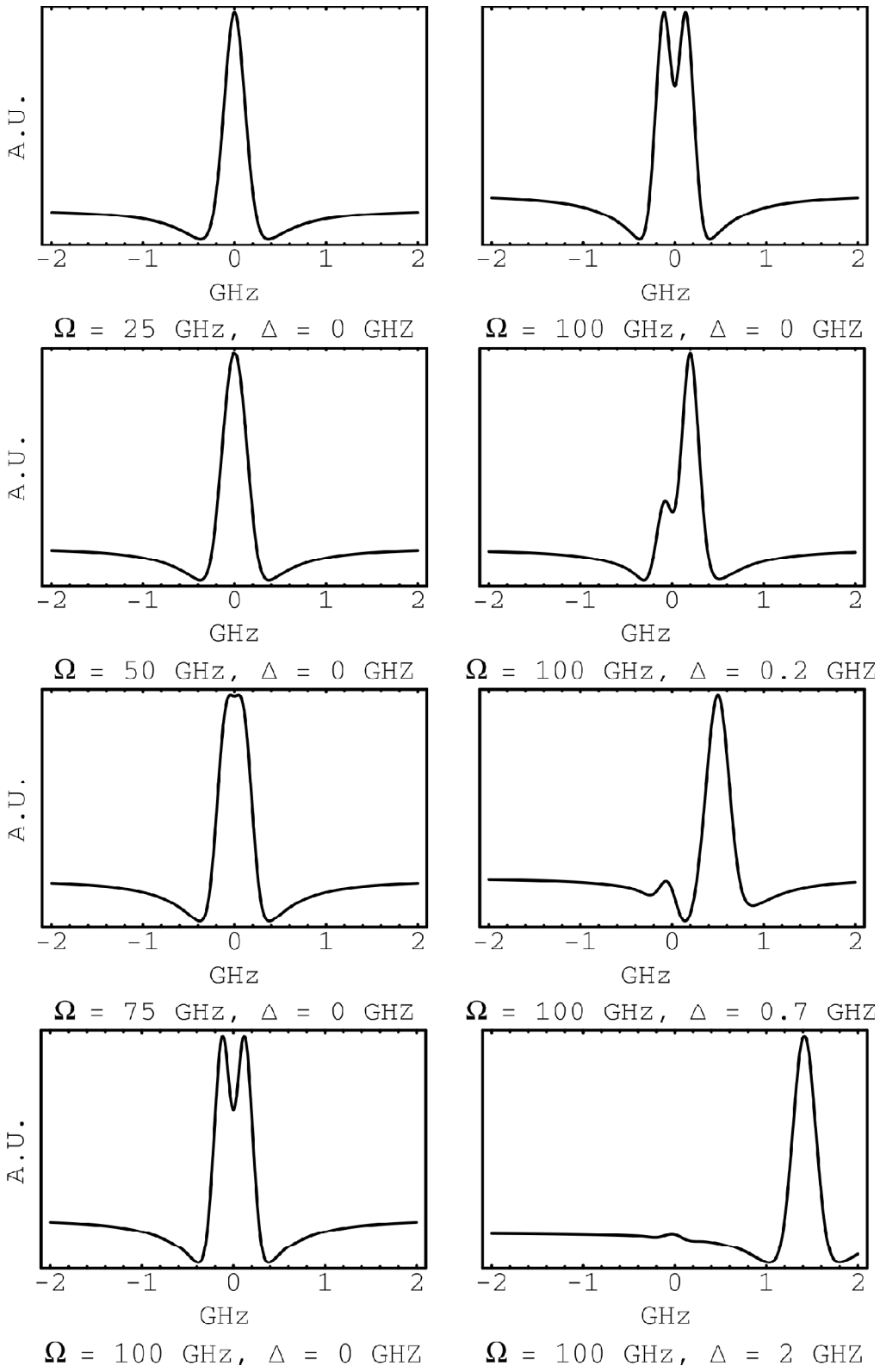

Figure 5: Nonlinear absorption spectrum $\delta\mathcal{P}_{\mu}(\Delta_{\mu})$ at different Ω and Δ

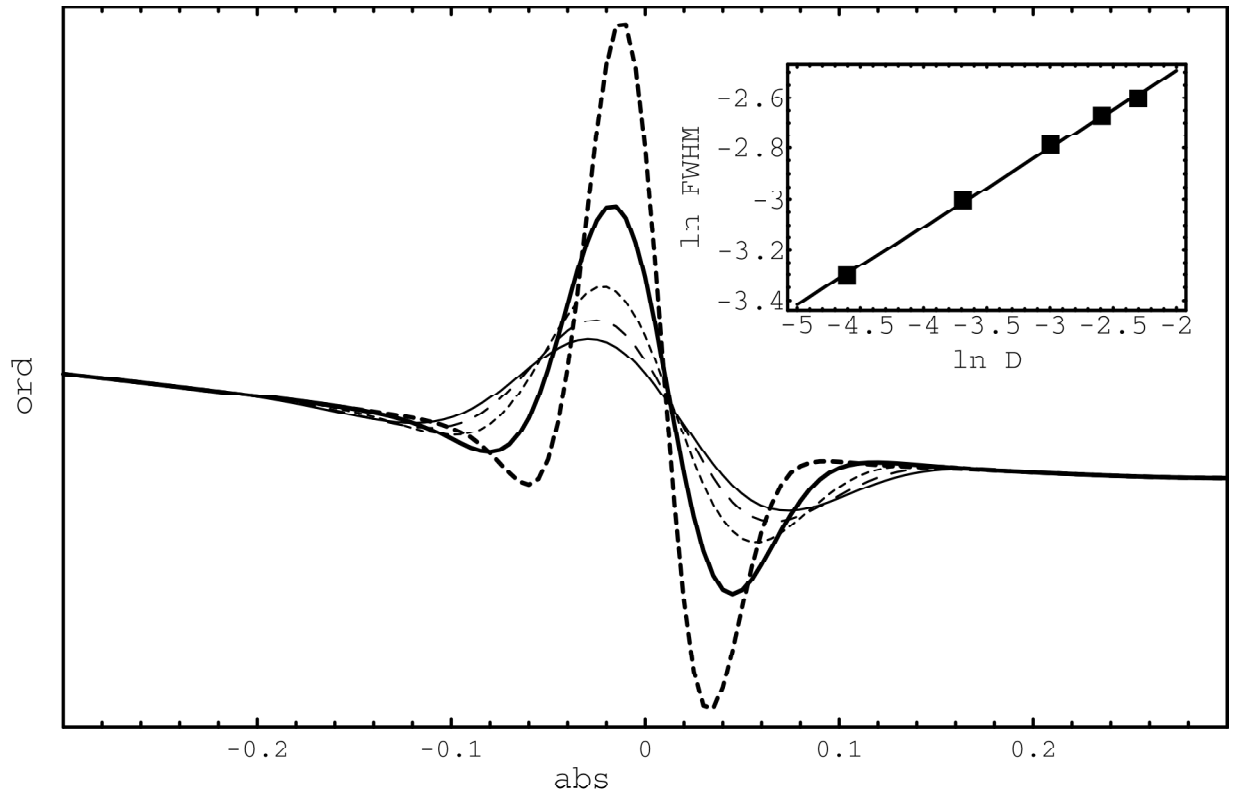

Figure 6: Peak of higher spatial harmonics at $\Gamma_\nu = \Gamma_\mu = 1$ GHz and different diffusion coefficient D. The peak grows up with D: $D / D0 = 0.1, 0.075, 0.05, 0.025, 0.001$, where $D_0 = 10^{13}$ m^2 / s^3. Inset: the width of peak as a function of diffusion coefficient in logarithmic coordinates

The broadening takes place because of the dephasing of wave in the reference frame of the excited ion due to the Coulomb scattering. At time t the active ion is scattered by ions at ground state by random angle ϑ. Its average value is zero $\langle\vartheta\rangle = 0$, while mean square value is nonzero in accordance with the diffusion law $\langle\vartheta^2\rangle = \nu t$. The ion started in the antinode of standing wave and having zero projection of the velocity onto the wavevector acquires velocity $\delta v \sim (\nu t)^{1/2} v_T$, then passes the distance $\delta x \sim \nu^{1/2} t^{3/2} v_T$. When the phase incursion of n-th harmonics reaches π the ion leaves the node, and then the effect of n-th harmonics vanishes. The characteristic duration of this process is of the order of $t \sim (nkv_T)^{-2/3}\ \nu^{-1/3}$. The central resonance is the consequence of even harmonics $n = 2, 4,...$ For estimation we take $n = 2$, then the broadening is $\delta\Delta_\mu \sim D^{1/3} k^{2/3}$. At $\delta\Delta_\mu \sim \Gamma_\mu$ the dip (in resonance case) is washed off and the peak (in nonresonance case) becomes wider. Notice that the considered effect of Coulomb dephasing corresponds to the density dependence $N^{1/3}$, while the known effect of Coulomb broadening of the Lamb dip gives $N^{1/2}$ [34]. The main peak at $\Delta_\mu = k_\mu \Delta / k$ experiences the common Coulomb broadening [23].

III. NUMERICAL CALCULATION

Three level scheme shown in Fig. 1 is studied numerically in this section. In the previous section we neglect the population of intermediate level m, and then take into account only the population of the final level l. This approximation answers the experimental conditions in ArII spectrum, where the initial state $|n\rangle = 4s\ ^2P_{1/2}$ is relatively wide, when the intermediate and final states $|m\rangle = 4p\ ^2S_{1/2}$, $|l\rangle = 3d\ ^2P_{3/2}$ are narrow: $\Gamma_n \approx 3\times10^9\ s^{-1}$, $\Gamma_m \approx 1.5 \times 10^8\ s^{-1}$, $\Gamma_l \approx 8\times10^7 s^{-1}$. The populations of these states are nearly $N_n \approx 10^9$ cm^{-3}, $N_m \approx 5 \times 10^9$ cm^{-3}, $N_l \approx 10^{11}$ cm^{-3}, then $N_n, N_m << N_l$.

If only level l is populated, then the calculation comes to the solution of equations (4) for polarizations of allowed transition ml and forbidden transition nl. Small-angle Coulomb scattering with velocity changing turns the set to the coupled Fokker — Plank equations. Its solution [24, 25] enables one to interpret the broadening of higher

harmonics resonance. Unfortunately, there was no quantitative agreement with experiment. In order to provide the agreement we present the numerical calculations taking into consideration the population of intermediate level m along with population ρ_n and polarization ρ_{mn} of the transition interacting with the strong standing wave [26].

(A) Method

After expansion the elements of density matrix to Fourier series (6) Eq.(1) yields a set of differential-difference equations for transition interacting with the standing wave

$$\begin{aligned}
&\left(ipkv + \Gamma_j - \hat{S}\right)\rho_j(p) \pm i\Omega[r_{mn}(p-1) + r_{mn}(p+1)]_{as} = q_j\delta_{p0}, \\
&\left(ipkv + \Gamma_{nm} - i\Delta - \hat{S}\right)r_{mn}(p) - i\frac{\Omega}{2}[N_{mn}(p-1) + N_{mn}(p+1)] = 0,
\end{aligned} \tag{8}$$

where $N_{ij} = \rho_i - \rho_j$, q_j is the excitation rate of level j, index "as" denote that the expression in the square brackets is to be antisymmetrized with respect to p: $[f(p)]_{as} = \frac{1}{2}[f(p) - f(-p)]$. For transitions ml and nl the following separate equations are derived:

$$\begin{aligned}
&\left(ipkv + \Gamma_1 - \hat{S}\right) r_{ml}(p) - i\frac{\Omega}{2}[r_{nl}(p-1) + r_{nl}(p+1)] = i\Omega_\mu N_{ml}(p), \\
&-i\frac{\Omega}{2}[r_{ml}(p-1) + r_{ml}(p+1)] + \left(ipkv + \Gamma_2 - \hat{S}\right)r_{nl}(p) = i\Omega_\mu r^*_{mn}(p).
\end{aligned} \tag{9}$$

The right-hand sides of (9) include population ρ_m and polarization r_{mn} in transition mn found from (8).

Each equation (8) couples three neighbor spatial harmonics. The source term in the right side is present only for $p = 0$. The equations for odd harmonics of populations and even harmonics of polarizations have no right parts, consequently they have zero solution. Thus, only the even harmonics of populations and even harmonics of polarizations have nonzero values. The analogous reasoning for Eq. (9) results in conclusion that the polarization r_{ml} of allowed transition involves only even harmonics, while the polarization of forbidden transition involves only odd harmonics.

Replacing the collision operator $\hat{S}$ by the finite-difference expression we get the infinite linear sets of algebraic equations from (8) and (9) with block-tridiagonal matrices. The blocks are formed by elements with equal velocity, while the number of harmonics passes along the whole band of values. Breaking the Fourier series at some harmonic and setting the increment δv for the velocity we obtain a finite algebraic set. The set can be solved by the matrix marching technique [35]. The boundary conditions are zero at the both ends of the velocity interval.

(B) Comparison with Experiment

Nonlinear spectrum at different values of the effective collision frequency is shown in Fig. 7. According to the sign in formula (7) the upwards direction in the plot corresponds to the better transmission, the downwards direction is absorption. Then the central dip can be interpreted as a splitting of the electromagnetically induced transparency peak. At $\Delta = 0$(a) the nonlinear resonance of the higher spatial harmonics appears as the dip. Outside the resonance (b) it reveals itself as a peak at $\Delta_\mu = 0$. Both near resonance and beyond the resonance the dip or peak in the center becomes wider with the collision frequency ν. At $\nu > 6 \times 10^6\, s^{-1}$ the dip is washed away and the peak substantially broadens.

For experimental scheme with the wide initial level $\Gamma_n >> \Gamma_{m,l}$ the "forbidden" transition appeared to be wider than the allowed transition by an order of magnitude, i.e. $\Gamma_{nl} >> \Gamma_{ml}$. It is the property of experimental scheme allowing observation of distinctive resonance of the higher spatial harmonics. At absence of the velocity changing

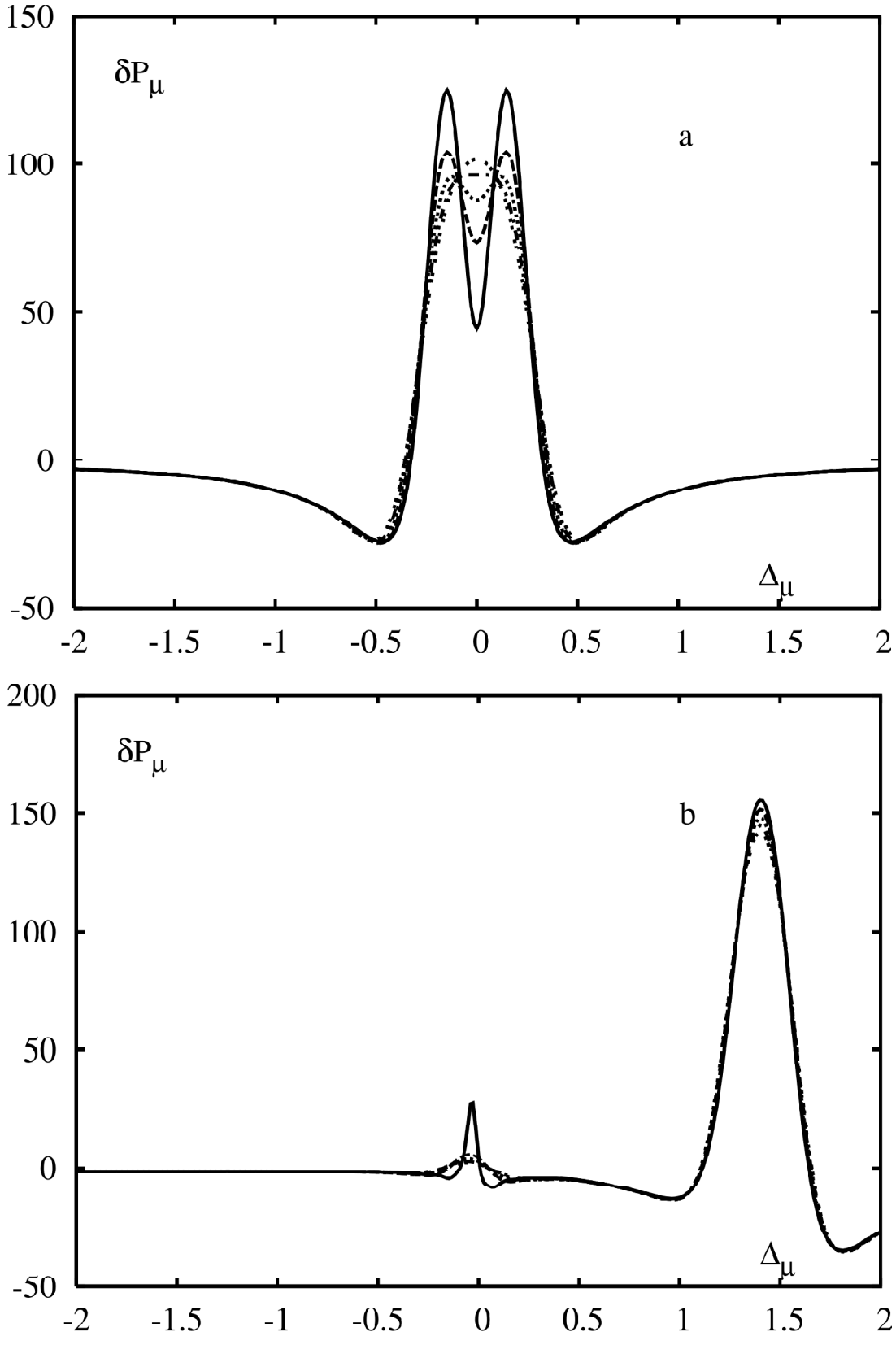

Figure 7: Nonlinear absorption spectrum $\delta\mathcal{P}_\mu(\Delta_\mu)$ (arb. units). Probe-field detuning Δ_μ is measured in GHz. Parameters choosen are $N_l = 10^{11}$ cm^{-3}, $N_m = N_n = 0$, $\Omega = 350$ MHz, and different collision frequencies: $\nu = 0$ (solid curve), 2×10^6 s^{-1} (dashes), 4×10^6 s^{-1} (frequent dots), 6×10^6 s^{-1} (dot-dashed), 8×10^6 s^{-1} (rare dots). (a) resonance case $\Delta = 0$, (b) non-resonance case $\Delta = 2$ GHz

collisions and the Stark broadening, within the applicability domain of the perturbation theory the dip has width $\Gamma_{ml} = (\Gamma_m + \Gamma_l) / 2$ of the allowed transition. The peak of EIT has width $\Gamma_{nl} = (\Gamma_n + \Gamma_l) / 2$ of the forbidden transition which is greater. The velocity changing collisions broaden the dip. The dip becomes less contrast and vanishes at higher collision frequencies.

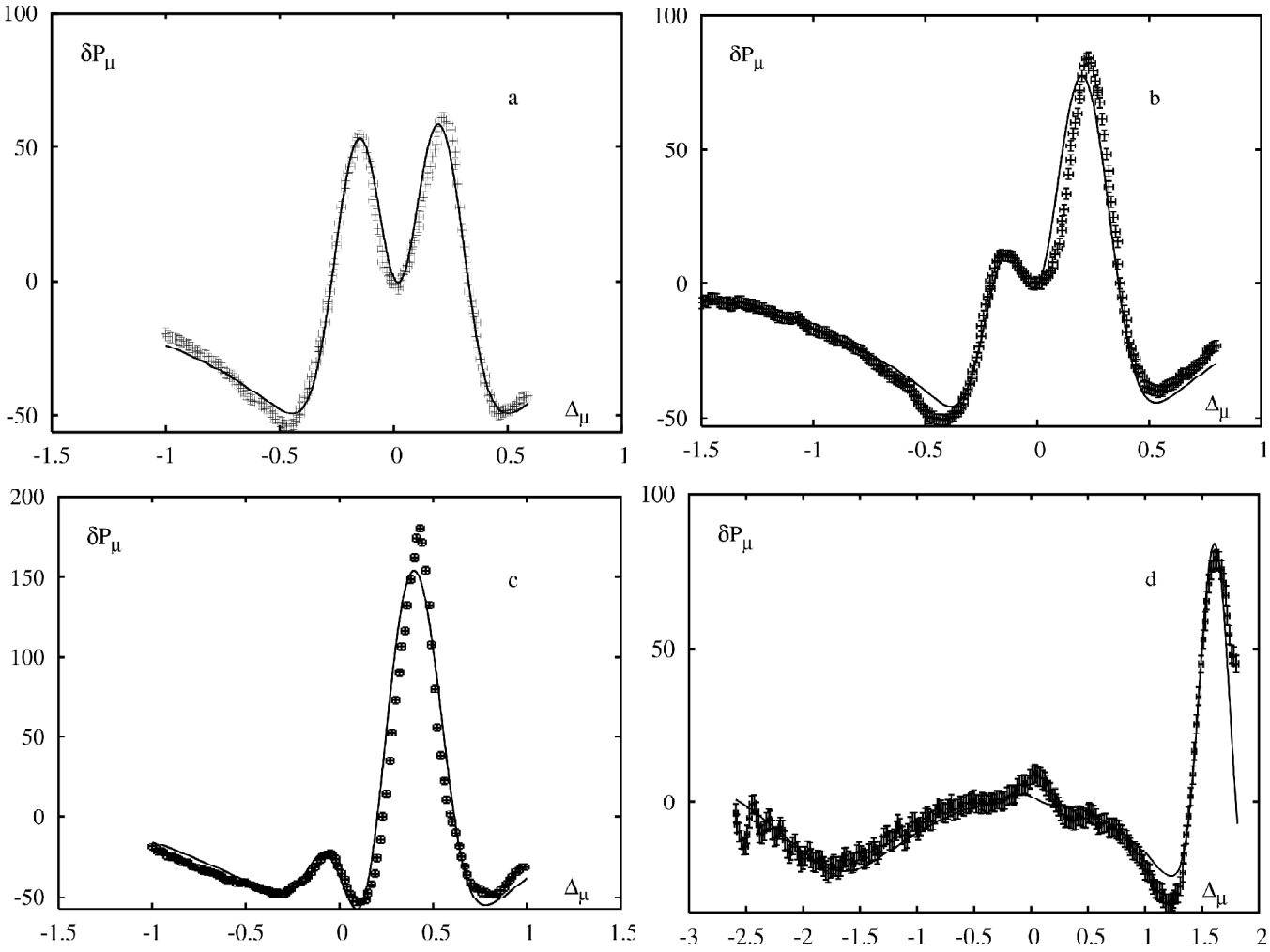

Figure 8: Nonlinear absorption $\delta\mathcal{P}_\mu$ (arb. units) as a function of probe-field detuning Δμ (GHz): experimental data (dots) and least-square fitting (curve)

To compare the computations with experiment the nonlinear spectra are fitted with the least square method. The set of linear equations (8), (9) includes 13 parameters: N_j, Γ_j, the unperturbed population and the width of level $j = n, m$, Γ_{ij}, the homogeneous width of transition ij ($i, j = n, m, l$). The detunings of strong and probe fields are Δ, Δ_μ k, k_μ are the wavenumbers of strong and probe fields, Ω, the Rabi frequency of strong field, ν, the effective frequency of ionic scattering. Two auxiliary parameters are appended, they are uncontrollable shifts of abscissa and ordinate axes. Absolute values of absorbed power was not measured, then one more auxiliary parameter appears, the amplitude of spectrum. Thus, there are 16 parameters, 13 of them are physical and 3 are auxiliary. The detuning Δ_μ plays a role of the independent variable. The greater part of parameters are known from independent measurements $\Gamma_m = 24$ MHz, $\Gamma_n = 480$ MHz, $\Gamma_{nm} = 280$ MHz, $\Gamma_{nl} = 300$ MHz, $\Gamma_{ml} = 50$ MHz, $kv_T = 4.9$ GHz, $k_\mu v_T = 3.46$ GHz, $N_m = 6 \times 10^9$ cm^{-3}, $N_n = 5 \times 10^8$ cm^{-3}, $N_l = 10^{11}$ cm^{-3}. The least-square fitting is carried out by 3 physical parameters: the effective frequency of ionic scattering ν, the Rabi frequency of strong field Ω, and the driving field detuning Δ. Nonlinear resonances at different Δ are shown in Fig. 8 along with the results of fitting. Sub-figure a–d are plotted at different detunings Δ: from resonance to nonresonance case.

Table 1
Fitted Parameters

	a	*b*	*c*	*d*
Δ (MHz)	13	153	450	2350
Ω (MHz)	380	320	330	350
ν (10^6 s^{-1})	2.0	3.6	6.9	2.5

Parameters found from the fitting are gathered in table I. All the measurements [18] were carried out at the same power of standing wave, but different strong field detuning. The spread of parameters in the table can be considered as a measure of possible systematic error or unaccounted factors in the theoretical model. Let us compare the fitted parameters to literature. The detuning measured in [18] were $\Delta = 0$, 200, 700, 2000 MHz, respectively. The uncertainty at frequency measurement was 100–150 MHz. The difference between fitted and measured data is likely explained by lens effects. Linear lens effect means the refraction of laser beam in plasma column due to nonuniform radial distribution of the ionic density together with the refractive index. There is a nonlinear effect, too. The nonlinear lens is a result of saturation effect and nonuniform radial distribution of the light intensity in the beam. The refractive indices of linear and nonlinear lenses depend on frequency, that leads to additional asymmetry of spectral profiles [36].

Obtained values of the Rabi frequency in theory $\Omega \approx 350$ MHz and in experiment $\Omega = 200$ MHz differ essentially. Note that in paper [18] other normalization of the Rabi frequency had been used, then the values presented were twice less (100 MHz). This discrepancy can be explained by inaccurate knowledge of the dipole moment of the transition [37]. The variation of effective diameter of the Gaussian laser beam along the discharge also pays its contribution to the discrepancy.

The effective collision frequency can be estimated from formula (5). At $N = 10^{14}$ cm^{-3} for singly charged ions we get $\nu = 10^7$ s^{-1}. For plot Fig. 8 (c) the fitted frequency agrees with the estimation, whereas resonance plots (a), (b) and nonresonance plot (d) the frequency obtained turns to be $2 \div 3$ times less. Such a wide spread of values can be explained by the small sensitivity of the width to the ionic density $\delta\Delta_\mu \sim \nu^{1/3}$. The errors of the absorbed power measurement also pay their contribution. Compare left and right scales in Fig. 4 we see the depth of higher spatial harmonic resonance is of the order of 1% of the absorbed power. Although the detection of nonlinear addition in experiment was provided by a synchronous detection, the spread still remained wide. One more reason of the discrepancy is imprecise knowledge of the relaxation constants. The natural widths are known comparatively well while the constants of electron deactivation and the Stark broadening of argon ionic transition are studied with less accuracy. The discrepancy betwen computation and measurement at *mn* transition reaches 30% [38, 39]. For *ml* transition between long-lived levels there are practically no data in literature, that is why the Stark broadening is not taken into account in the fitting procedure.

IV. CONCLUSIONS

Thus, the collisional shape of the higher spatial harmonic slow-atom resonance is calculated both numerically and analytically by the perturbation theory. The Coulomb broadening of the resonance is found in the 4th order of the perturbation theory neglecting the population of the intermediate level. It allows to interpret experimental data qualitatively. The numerical calculations take into consideration small population of the upper level and saturation in *mn* transition. It allows fitting the experimental data with accuracy $5 \div 10\%$, i.e. within the error limit. The agreement occurs at plasma and light parameters that are in agreement with known data.

Acknowledgements

Authors are grateful to S. A. Babin and D. V. Churkin for kindly presented experimental data, for E. V. Podivilov and M. G. Stepanov for helpful discussions. The work is partially supported by the Program "Optical spectroscopy and fre-quency standards" from the Physical Science Department of Russian Academy of Sciences and the Government program NSh-2979.2012.2.

References

[1] S. E. Harris, "Electromagnetically Induced Transparency," *Physics Today* **50**, 36–42, (1997).

[2] J. P. Marangos, "Electromagnetically Induced Transparency," *J. Mod. Opt.* **45**, 471–503, (1998).

[3] S. E. Harris, J. E. Field, and A. Imamoglu, "Nonlinear Optical Processes using Electromagnetically Induced Transparency," *Phys. Rev. Lett.* **64**, 1107–1110, (1990).

[4] M. Jain, H. Xia, G. Y. Yin, A. J. Merriam, and S. E. Harris, "Efficient Nonlinear Frequency Conversion with Maximal Atomic Coherence," *Phys. Rev. Lett.* **77**, 4326–4329, (1996).

[5] A. S. Zibrov, M. D. Lukin, and M. O. Scully, "Nondegenerate Parametric Self-oscillation via Multiwave Mixing in Coherent Atomic Media," *Phys. Rev. Lett.* **83**, 4049–4052, (1999).

[6] A. S. Zibrov, M. D. Lukin, D. E. Nikonov, L. Hollberg, M. O. Scully, V. L. Velichansky, and H. G. Robinson, "Experimental Demonstration of Laser Oscillation without Population Inversion via Quantum Interference," *Phys. Rev. Lett.* **75**, 1499–1502, (1995).

[7] J. Y. Gao, S. H. Yang, D. Wang, X. Z. Guo, K. X. Chen, Y. Jiang, and B. Zhao, "Electromagnetically Induced Inhibition of Two-photon Absorption in Sodium Vapor," *Phys. Rev. A* **61**, 023401, (1999).

[8] M. M. Kash, V. A. Sautenkov, A. S. Zibrov, L. Hollberg, G. R. Welch, M. D. Lukin, Y. Rostovtsev, E. S. Fry, and M. O. Scully, "Ultraslow Group Velocity and Enhanced Nonlinear Optical Effects in a Coherently Driven Hot Atomic Gas," *Phys. Rev. Lett.* **82**, 5229–5232, (1999).

[9] D. Budker, D. F. Kimball, S. M. Rochester, and V. V. Yashchuk, "Nonlinear Magneto-optics and Reduced Group Velocity of Light in Atomic Vapor with Slow Ground State Relaxation," *Phys. Rev. Lett.* **83**, 1767–1770, (1999).

[10] E. E. Mikhailov, Y. V. Rostovtsev, and G. R. Welch, "Group Velocity Study in hot ^{87}Rb Vapour with Buffer Gas," *J. Mod. Opt.* **50**, 2645 – 2654, (2003).

[11] S. Knappe, R. Wynands, J. Kitching, H. G. Robinson, and L. Hollberg, "Characterization of Coherent Population-trapping Resonances as Atomic Frequency References," *J. Opt. Soc. Am. B* **18**, 1545–1553, (2001).

[12] I. Novikova, A. B. Matsko, and G. R. Welch, "Large Polarization Rotation via Atomic Coherence," *Opt. Lett.* **26**, 1016–1018, (2001).

[13] C. Liu, Z. Dutton, C. H. Behroozi, and L. V. Hau, "Observation of Coherent Optical Information Storage in an Atomic Medium using Halted Light Pulses," *Nature* **409**, 490–493, (2001).

[14] D. F. Phillips, A. Fleischhauer, A. Mair, R. L. Walsworth, and M. D. Lukin, "Storage of Light in Atomic Vapor," *Phys. Rev. Lett.* **86**, 783–786, (2001).

[15] T. Chaneliere, D. N. Matsukevich, S. D. Jenkins, S. Y. Lan, T. A. B. Kennedy, and A. Kuzmich, "Storage and Retrieval of Single Photons Transmitted between Remote Quantum Memories," *Nature* **438**, 833–836, (2005).

[16] I. M. Beterov and V. P. Chebotaev, *Three-Level Gas Systems and Their Interaction with Radiation*, vol. 3 of *Progr. Quant. Electron.* (Pergamon Press, Oxford, 1974).

[17] S. G. Rautian and A. M. Shalagin, *Kinetic Problems of Non-linear Spectroscopy* (North-Holland, Amsterdam, Oxford, 1991).

[18] S. A. Babin, E. V. Podivilov, V. V. Potapov, D. V. Churkin, and D. A. Shapiro, "Nonlinear Resonance Induced by the Higher Spatial Coherence Harmonics," *Zh. Eksp. Teor. Fiz.* **121**, 807–818 (2002). [JETP, **94** (4) 694–703 (2002)].

[19] S. A. Babin, D. V. Churkin, E. V. Podivilov, V. V. Potapov, and D. A. Shapiro, "Splitting of the Peak of Electromagnetically Induced Transparency by the Higher-order Spatial Harmonics of the Atomic Coherence," *Phys. Rev. A* **67**, 043808, (2003).

[20] A. K. Popov, *Introduction to Nonlinear Spectroscopy* (Nauka, Novosibirsk, 1983). [in Russian].

[21] B. J. Feldman and M. S. Feld, "Laser-induced Line-narrowing Effects in Coupled Doppler-broadened Transitions. II. Standing-wave Features." *Phys. Rev. A* **5**, 899–918, (1972).

[22] S. A. Babin and D. A. Shapiro, "Spectral Line Broadening due to the Coulomb Interaction in Plasma," *Phys. Rep.* **241**, 119–216, (1994).

[23] S. A. Babin, M. G. Stepanov, D. V. Churkin, and D. A. Shapiro, "Coulomb Broadening of the Peak of Electromagnetically Induced Transparency in Plasma," Zh. Eksp. Teor. Fiz. **125**, 1092–1099 (2004). [JETP, **98** (5) 953–959 (2004)].

[24] O. V. Belai and D. A. Shapiro, "Coulomb Broadening of Nonlinear Resonances in a Field of Intense Standing Wave," Pis'ma v Zh. Eksp. Teor. Fiz. **79**, 257–261 (2004). [JETP Lett., **79** (5) 203–207 (2004)].

[25] O. V. Belai, D. A. Shapiro, and S. N. Yakovenko, "Spectrum of Nonlinear Absorption in the Weak Saturatimg Standing Wave," *Kvant. Elektr.* **25**, 1027–1032, (2005).

[26] O. V. Belai and D. A. Shapiro, "The Effect of the Ionic Level Population on the Nonlinear Resonances of Higher order Spatial Harmonics," *Opt. Spektr.* **100**, 971–978 (2006).

[27] S. Stenholm and W. E. Lamb, "Semiclassical Theory of High-intensity Laser," *Phys. Rep.* **181**, 618–635, (1969).

[28] B. J. Feldman and M. S. Feld, "Theory of High Intensity Gas Laser," *Phys. Rev. A* **1**, 1375–1396, (1970).

[29] S. G. Rautian and I. I. Sobel'man, "Radiation Emitted by Atoms Moving in the Field of a Standing Wave," *Zh. Eksp. Teor. Fiz.* **44**, 934–945, (1963). [Sov. Phys. JETP **17** (3) 635-642 (1963)].

[30] S. Stenholm, "Theoretical Foundation of Laser Spectroscopy," *Phys. Rep.* **43**, 151–221, (1978).

[31] A. M. Bonch-Bruevich, T. A. Vartanyan, and N. A. Chigir', "Subradiative Structure in the Absorption Spectrum of a Two-level System in a Biharmonic Radiation Field," *Zh. Eksp. Teor. Fiz.* **77**, 1899–1909, (1979). [Sov. Phys. JETP **50** (5) 901–906 (1979)].

[32] A. A. Mak, S. G. Przhibelskii, and N. A. Chigir, "Nonlinear Resonance Phenomena in Bichromatic Fields," *Izv. Acad. Nauk. SSSR, Ser. Fiz.* **47**, 1976–1983, (1983).

[33] S. Papademetriou, S. Chakmakjian, and J. C. R. Stroud, "Optical Subharmonic Rabi Resonances," *J. Opt. Soc. Am. B* **9**, 1182–1188, (1992).

[34] G. I. Smirnov and D. A. Shapiro, "Spectral Line Broadening due to Coulomb Interaction," *Zh. Eksp. Teor. Fiz.* **76**, 2084–2093, (1979). [Sov. Phys. JETP, **49** (6) 1054–1058 (1979)].

[35] A. A. Samarsky and A. V. Gulin, *Numerical Methods* (Nauka, Moscow, 1989). [in Russian].

[36] G. Stephan and M. Tr¨umfer, "Macroscopic Parameter and Line Shapes of a Gas Laser," *Phys. Rev. A* **40**, 1925–1939, (1984).

[37] A. Hibbert and J. E. Hansen, "Transitions in Ar-II," *J. Phys. B: At. Mol. Opt. Phys.* **27**, 3325–3347, (1994).

[38] S. Pellerin, K. Musiol, and J. Chapelle, "Measurement of Atomic Parameters of Singly Ionized Argon Lines — III. Stark Broadening Parameters," *J. Quant. Spectr. Radiat. Transf.* **57**, 377–393, (1997).

[39] J. A. Aparicio, M. A. Gigosos, V. R. Gonz´alez, C. P´erez, M. I. de la Rosa, and S. Mar, "Measurement of Stark Broadening and Shift of Singly Ionized Ar lines," *J. Phys. B: At. Mol. Opt. Phys.* **31**, 1029–1048, (1998).